

PAPER • OPEN ACCESS

Validation of Sentinel-1-derived sea ice cover data in the Arctic

To cite this article: Qiang Zhang *et al* 2020 *IOP Conf. Ser.: Earth Environ. Sci.* **502** 012032

View the [article online](#) for updates and enhancements.

You may also like

- [Integrating satellite-based forest disturbance alerts improves detection timeliness and confidence](#)

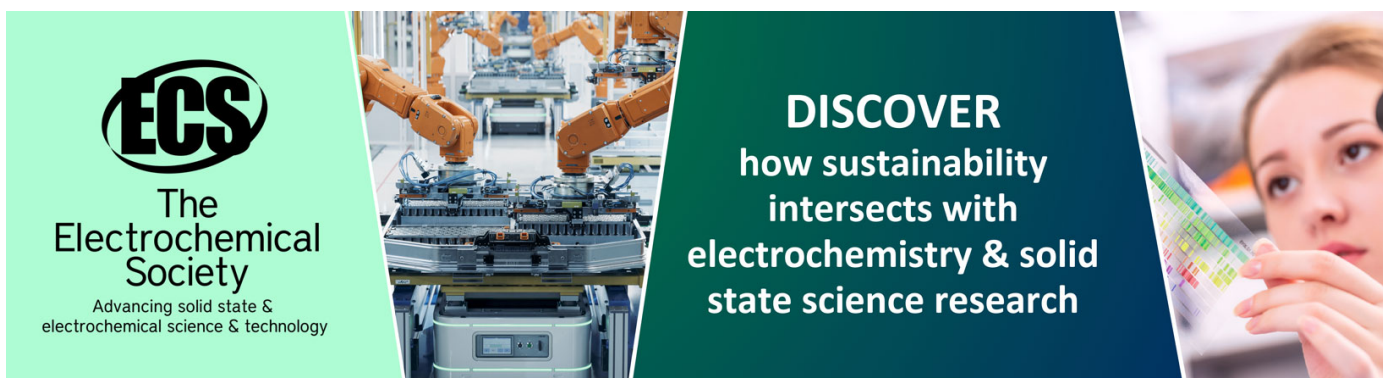
Johannes Reiche, Johannes Balling, Amy Hudson Pickens et al.

- [The role of sea ice in establishing the seasonal Arctic warming pattern](#)

Sergio A Sejas and Patrick C Taylor

- [Forest disturbance alerts for the Congo Basin using Sentinel-1](#)

Johannes Reiche, Adugna Mullissa, Bart Slagter et al.



ECS
The
Electrochemical
Society
Advancing solid state &
electrochemical science & technology

DISCOVER
how sustainability
intersects with
electrochemistry & solid
state science research

Validation of Sentinel-1-derived sea ice cover data in the Arctic

Qiang Zhang^{1,2}, Shibo Guo², Yan Sun², JianPing Dou³ and Xiao-Ming Li²

1. College of Geomatics and Geoinformation, Guilin University of Technology, Guangxi Guilin 541006, China
2. Key Laboratory of Digital Earth Science, Aerospace Information Research Institute, Chinese Academy of Sciences, Beijing, 100094
zqglut@163.com
3. Ecology and Environment Quality Control and Service Center of Zibo City, ShanDong, Zibo, 255000, China

Abstract. The Sentinel-1 synthetic aperture radar (SAR) instrument can image the polar regions with a large area and high temporal and spatial resolutions, which is particularly suitable for sea ice monitoring in the Arctic. In a previous study, a support vector machine (SVM)-based method was developed to automatically extract the sea ice cover from Sentinel-1 SAR Extra Wide (EW) swath mode data in cross-polarization (horizontal-vertical, HV, or vertical-horizontal, VH). For validation, 468 Sentinel-1 EW HV-polarized images acquired in the Arctic are used to derive the sea ice cover with a spatial resolution of 0.96 km. We then compared the SAR-derived sea ice cover with the Ice Mapping System (IMS) dataset, which has a resolution of 1.0 km, and the AMSR-2 sea ice concentration (SIC, 15% is used as a threshold for deriving sea ice cover) dataset, which has a resolution of 3.125 km, based on pixel-by-pixel matching. The accuracies of the comparisons with the IMS and SIC data are 85.01% and 88.69%, respectively. The comparison shows that the IMS dataset is mostly overestimates the sea ice cover, while the AMSR2 dataset is relatively underestimates the sea ice extent. On the other hand, the sea ice cover information derived from the Sentinel-1 images by using the proposed method well characterizes the details of the marginal ice zone (MIZ). Furthermore, through the analysis of individual cases, the main factors that affect accuracy are drift (or pack) ice and a high land proportion in some areas.

Keywords: Sea ice cover; Sentinel-1; SAR; IMS; AMSR-2

1. Introduction

Sea ice is one of the important factors affecting the polar, and even global, climate system, which has been the focus of climate researchers[1] In addition, with the melting of sea ice in the Arctic, the strategic significance of Arctic shipping routes, mineral and fishery resource development are becoming increasingly important[2]. To better study the Arctic, varieties of Arctic environment datasets have been produced. The main types of datasets related to sea ice are sea ice concentration and sea ice cover datasets. Sea ice concentration datasets are mainly obtained by inversion based on brightness temperature data of passive microwave radiometers [3-5]. Sea ice cover datasets can be derived from sea ice concentration datasets [6]. It is also possible to obtain the sea ice cover through visible-infrared sensors [7] and active microwave sensors such as synthetic aperture radar (SAR). We propose a novel method of deriving sea ice cover data by using Sentinel-1 SAR imagery acquired in



cross-polarization [8]. Some studies have shown that the accuracies of each sea ice cover dataset are different [9-10]. In this study, our sea ice cover products were compared with the sea ice concentration dataset from the University of Bremen and the sea ice cover dataset from the National Ice Center of United States to analyze the difference and accuracy of each dataset.

2. Data & Methods

2.1 Data

2.1.1 Sea ice cover data derived from Sentinel-1 (SIES1)

The Sentinel-1 (S1) imagery used in this study is Extra Wide (EW) swath mode cross-polarization (horizontal-vertical, HV) Level-1 Ground Range Detected (GRD) images, which were mainly acquired in the Arctic marginal ice zone (MIZ) from July 1 to September 30, 2018 (see Figure 1).

In our previous study, a support vector machine (SVM)-based method was developed to automatically extract the sea ice cover from these S1 images. In this paper, 468 sea ice cover data (SIES1) are produced from the S1 EW HV-polarization images by using this method. Figure 1 shows the spatial distribution of the 468 S1 images in the Arctic MIZ, in which boxes of various colors represent the images from different dates. SIES1 data have a high spatial resolution of 0.96 km and can be obtained in real time once the SAR image is acquired. SIES1 data mark land, water and ice with values of -1, 1 and 0, respectively.

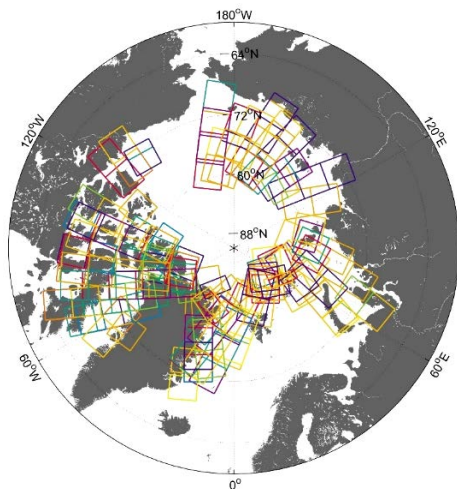


Figure 1. Spatial distribution of 468 S1 SAR images acquired from July 1 to September 30, 2018. (various colors represent images from different dates).

2.1.2 IMS sea ice extent dataset (IMS)

Interactive Multisensor Snow and Ice Mapping System (IMS, <https://nsidc.org/data/G02156/versions/1>) sea ice extent data produced by the National Snow & Ice Data Center (NSIDC) are used for comparison with the SIES1 data. The sea ice information derived from the passive microwave (radiometer), active microwave (SAR) and optical (multiple spectra) remote sensing sensors, as well as in situ data, are used to produce the IMS sea ice cover product[11]. These data are updated daily. In this study, the IMS data at a spatial resolution of 1 km is used for comparison. IMS marks “no data”, water, land, ice and snow covered land, with values of 0, 1, 2, 3 and 4, respectively.

2.1.3 AMSR-2 Sea ice concentration dataset (AMSR2)

The sea ice concentration refers to the proportion of sea ice in a unit area, ranging from 0 to 100, and is one of the basic parameters for characterizing the sea ice cover. The daily sea ice concentration

product with a resolution of 3.125 km released by the University of Bremen, Germany, is selected as another data source, and the selected product is the recent ASI data, version 5.4[12].

2.2 Comparison of Methods

Following the introduction above, the focus of this paper is on evaluating the accuracy of the SIES1 data, based on comparisons with the IMS and AMSR2 data. The comparisons are conducted on a spatial and temporal matchup with the pixels of the IMS and AMSR2 datasets using nearest-neighbor collocation.

After finding the closest IMS and AMSR2 data in time, the SIES1 is compared by a pixel-by-pixel-based nearest-neighbor matching across longitude and latitude, while the former two datasets are recognized as the “true” sea ice conditions. The basis of this processing is to keep the three datasets at the same resolution level. The SIES1 and IMS data have very similar spatial resolutions of 0.96 km and 1.0 km, respectively, but the AMSR2 data have a resolution of 3.125 km. Thus, a downsampling operation needs to be performed on the SIES1 data prior to matchup. Figure.2 shows the resampling illustration that using a modal analysis operator. In the 3×3 grids, a value of 0 appears 5 times and is the maximum count; therefore, the resampled grid is set to 0. The SIES1 data are downsampled to a resolution of 0.96×3 km (equal to 2.88 km).

For the evaluation, we use the matching accuracy (*MA*) as a validation parameter. The correctly matched sea ice and open water pixels are recorded as n_{ice_match} and n_{water_match} , respectively. Then, the accuracy is defined as follows:

$$MA = \frac{n_{ice_Match} + n_{water_Match}}{n_{total}} \cdot 100\% \quad (1)$$

where n_{total} denotes the total number of grid cells in one SIES1 image.

Furthermore, the AMSR2 sea ice concentration data have values ranging from 0 to 100 in each grid, which refers to the proportion of sea ice in a unit area. In this paper, we take 15% as a threshold for the identification of an ice grid[13]. In other words, if the value of one grid is larger than 0.15, the grid is thought to be filled with ice. Then, the match is conducted based on this value.

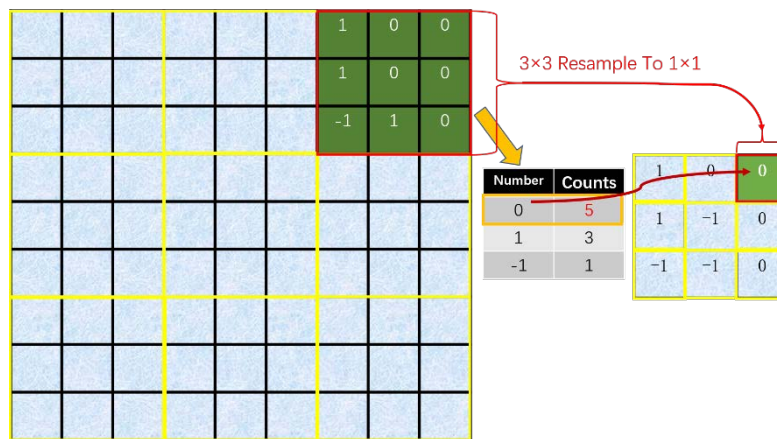


Figure 2. Resampling and segmentation of the label assignments.

3. Results & Analysis

In this study, 60,060,327 data points from the 486 SIES1 images were collocated with the IMS data, among which 51,057,112 points were correctly matched. The overall matching accuracy was 85.01%. In total, 6,376,611 points were collocated with the AMSR2 data, among which 5,655,363 points were correctly matched, with an overall matching accuracy of 88.69%. The results verify the reliability of

these data. Then, some of the features are found by analyzing the data-matching accuracy of every image in both time and space. In the following statement, the matching accuracy of the SIES1 and IMS data was denoted by MA_{IMS} and that of the SIES1 and AMSR2 data was denoted by MA_{AMSR2} . Figure 3 shows the scatter plot of the relative relationship between the MA_{IMS} and MA_{AMSR2} values in the 486 images, in which most of the accuracies are concentrated above 80%. One can see that there are far more points above the red line than below the red line, which indicates that the SIES1 data are closer to AMSR2 data than to the IMS data. Taking the original S1 image as the evaluation standard, the SIES1 data are relatively close to the AMSR2 data, which may indicate that the AMSR2 data can better describe the actual sea ice cover than the IMS data.

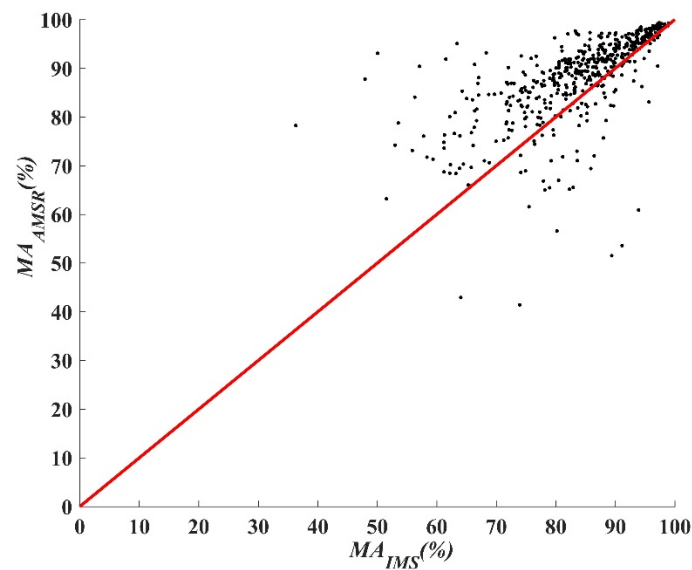


Figure 3. Scatter plot of the MA_{IMS} values versus the MA_{AMSR2} values.

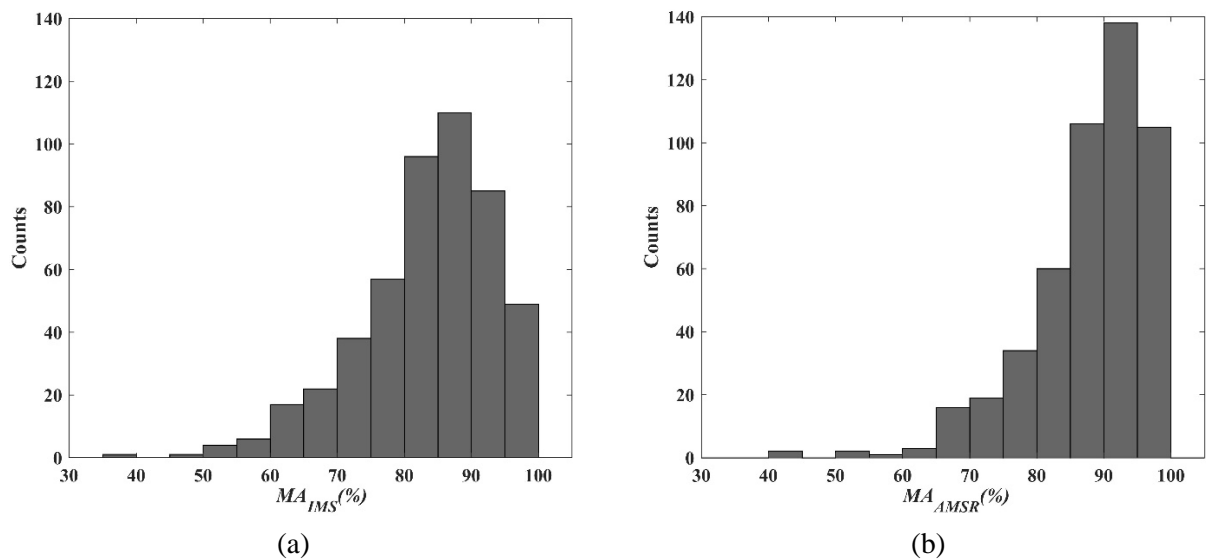


Figure 4. Frequency distribution of MA_{IMS} (a) and MA_{AMSR2} (b)

Figure 4a and Figure 4b show the probability distribution of the MA_{IMS} and MA_{AMSR2} values of the 486 images, respectively. Among them, the MA_{IMS} with the highest frequency in Figure 4a is between

85-90%, and 81% of the MA_{IMS} values are between 75%-100%, while the MA_{AMSR2} with the highest frequency in Figure 4b is between 90%-95%, and 84% of the MA_{AMSR2} values are between 80%-100%. Compared with the former, MA_{AMSR2} is more concentrated. Although the above comprehensive analysis shows that the AMSR2 data yield better matching results, it should be noted that they are obtained under different resolutions. The resolution of IMS is approximately three times higher than that of AMSR2, which is an important reason why the MA s of the AMSR2 data are better than those of the IMS data.

3.1 Temporal Analysis

Figure 5a and Figure 5b show the boxplots for the distributions of the matching accuracies of the IMS and AMSR2 data during July 2 - September 30, 2018, every 9 days. There was no obvious correlation between the MA distribution and time. However, the MA_{IMS} values from August had a large fluctuation range and high dispersion, while MA_{AMSR2} values are more stable at all time points.

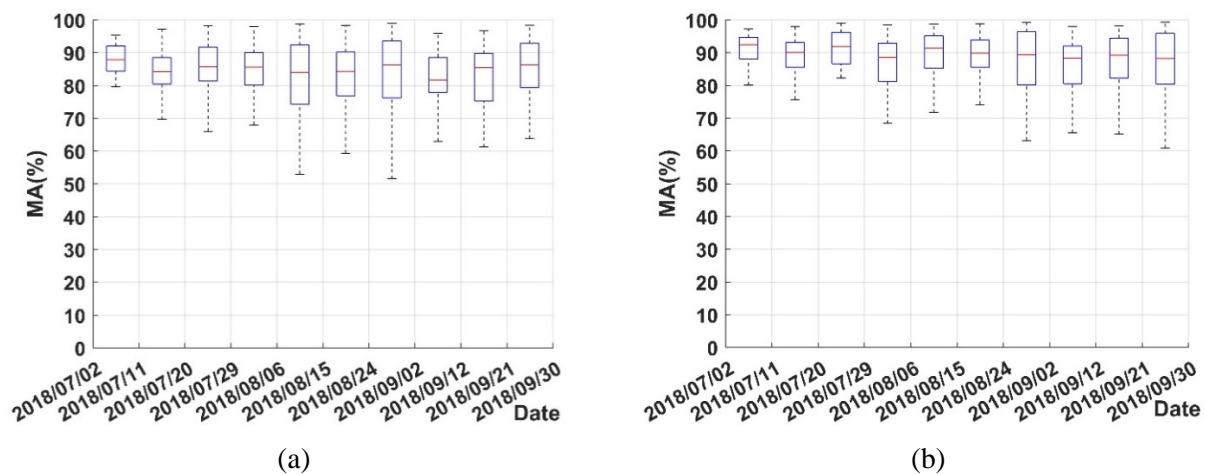


Figure 5. The distributions of the MA_{IMS} (a) and MA_{AMSR2} (b) values for July 2 -September 30, 2018.

3.2 Spatial Analysis

As shown in Figure 6, to study the differences in the spatial distributions of the MA values, the regions covered by the data with a matching accuracy less than 80% are shown in red. Both the IMS and AMSR2 data show that the data distribution with low matching accuracy values is obviously regional. Low matching accuracy values are mainly distributed in northeast of the East Siberian Sea, the Fram Strait, the Greenland Sea, Baffin Bay, the Davis Strait and the Canadian Arctic Archipelago (CAA). In addition, the matching accuracy values of different products in the same region are also different. It is obvious that the coverage with low MA_{IMS} values is larger than that of the MA_{AMSR2} values.

Based on the specific analysis and research on the red areas above, we can divide them into two categories:

- Regions where the growth and disappearance of drift (or pack) ice at the MIZ are quite drastic. It mainly includes the Fram Strait, the Greenland Sea, Baffin Bay, the Davis Strait and the area northeast of East Siberian Sea.
- Regions where sea ice is located in the area of a narrow strait, which mainly includes the Canadian Arctic Archipelago.

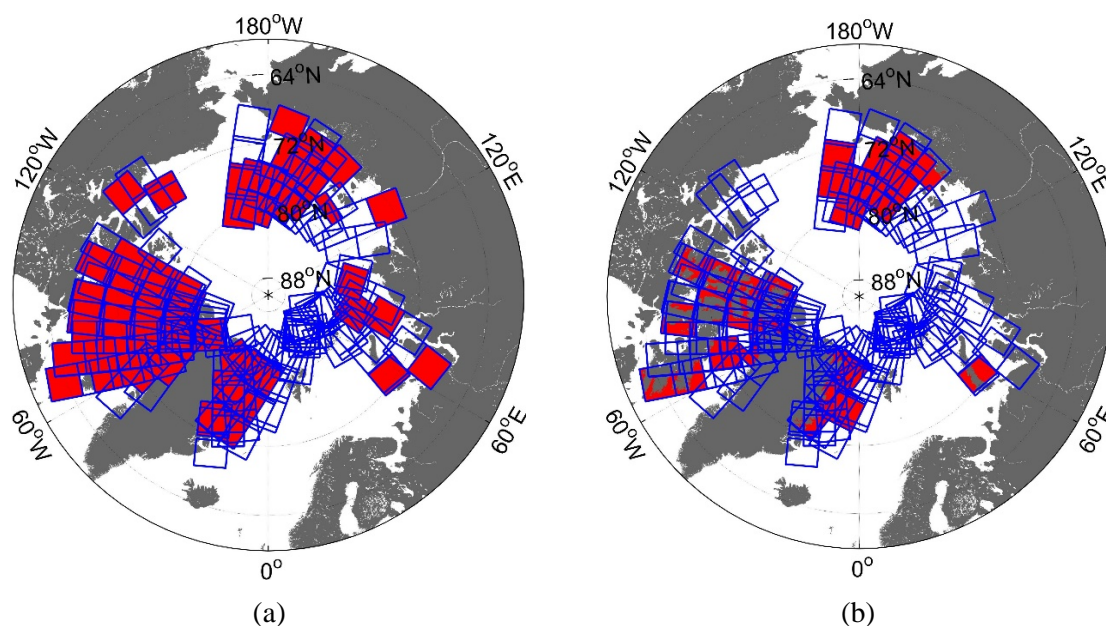
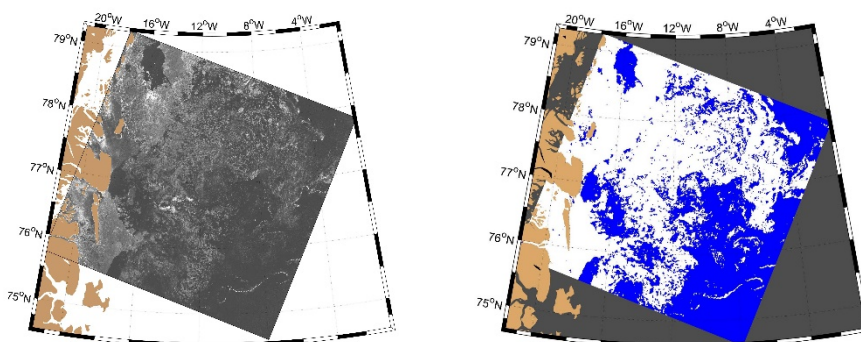


Figure 6. Areas where the MA_{IMS} (a) and MA_{AMSR2} (b) values are less than 80%.

The following selected representative data are taken as examples to illustrate the cause of low matching accuracies.

3.2.1 Cases of the Fram Strait and the area northeast of the East Siberian Sea

The Fram Strait is an important link between the Arctic Ocean and the North Atlantic Ocean, and it is the main outlet for Arctic drift ice in summer [14]. Sea ice has a strong dynamic effect in this region. Figure 7 shows an S1 HV-polarization EW mode SAR image from July 21, 2018, located in the Fram Strait. Figure 7a is the calibrated and denoised backscatter image, and Figure 7b is the SIES1 product derived from Figure 7a, in which white pixels represent sea ice and blue pixels represent water. The SIES1 data are matched to the IMS data (Figure 7c) and the AMSR2 data (Figure 7d). The white and blue areas represent the correctly matched pixels of sea ice and open water, respectively, in the two comparisons. The red area indicates that the pixels of SIES1 are open water but are recognized as sea ice in the IMS/AMSR2 data, while the pink area indicates the opposite results. Comparing Figure 7c to Figure 7d, we find that the AMSR2 has higher MA values than the IMS data, especially in the description of the MIZ, which indicates that a 15% concentration is a reasonable threshold to estimate the sea ice cover or extent. The large red areas in Figure 7c indicate that the amount of sea ice cover in the IMS data is much larger than that in the SIES1 data. Referring to the original S1 image, the sea ice cover of the IMS data for this case is highly overestimated.



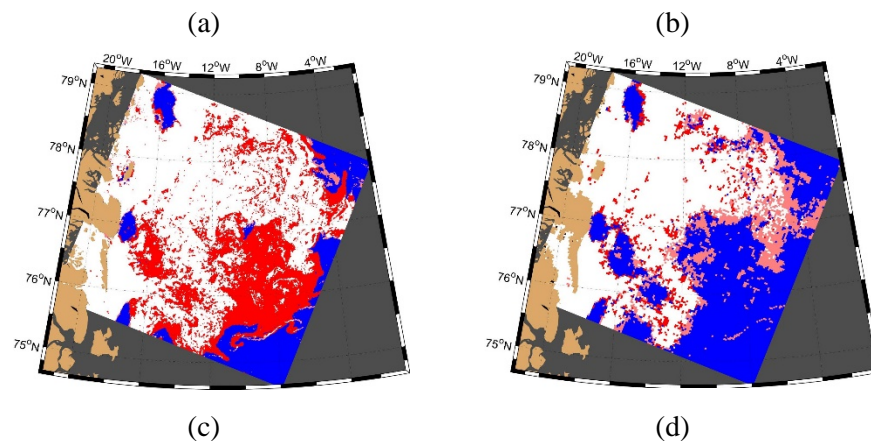


Figure 7. An example of an S1 image (a) and its derived sea ice cover (b) over the Fram Strait and its comparison with the IMS (c) and AMSR2 data (d).

3.2.2 Case of the East Siberian Sea

The East Siberian Sea is mainly affected by land runoff and solar radiation in summer, which provides continuous heat for the melting of sea ice. Figure 8a shows an image from September 12, 2018, located in the area northeast of the East Siberian Sea. Through the comparison of Figure 8c and Figure 8d, it can be found that both the MA_{IMS} and MA_{AMSR2} values are not very high. The large pink region in Figure 8d indicates that the sea ice coverage of the AMSR2 data is greatly underestimated. In Figure 8c, by comparing the IMS data with the original SAR image, we find that the interstitial waters in the original image are also considered sea ice in the IMS data. This finding indicates that the sea ice cover of the IMS data is overestimated. However, the IMS data still give a realistic picture of the MIZ.

Drift (or pack) ice is the main resource of the low matching accuracy values of the above sea areas. First, thin and discrete drift (or pack) ice occurs far offshore in a wide area. The IMS products are mainly obtained by artificial interpretation based on multisource data. Once ice is detected in a fixed area (1 km*1 km in the IMS data), this grid area is set to sea ice. Thus, the sea ice cover of the IMS in drift ice areas can be easily overestimated. The sea ice cover of the AMSR2 data is obtained from the retrieved bright temperature data. Considering that the bright temperature of thin drift ice is close to that of the surrounding water and the threshold of the ice concentration is set to 15%, some drift ice may be misclassified as water in AMSR2 products, which causes the underestimation of the sea ice extent. Second, drift (or pack) ice can be easily affected (moved or melted) by temperature, ocean currents and wind fields. The area and location of sea ice cover varies greatly in one day, which makes it difficult to determine the sea ice extent in these areas. Therefore, the SIES1 data obtained from real-time SAR data may overestimate and underestimate the sea ice extent when matching the two daily datasets.

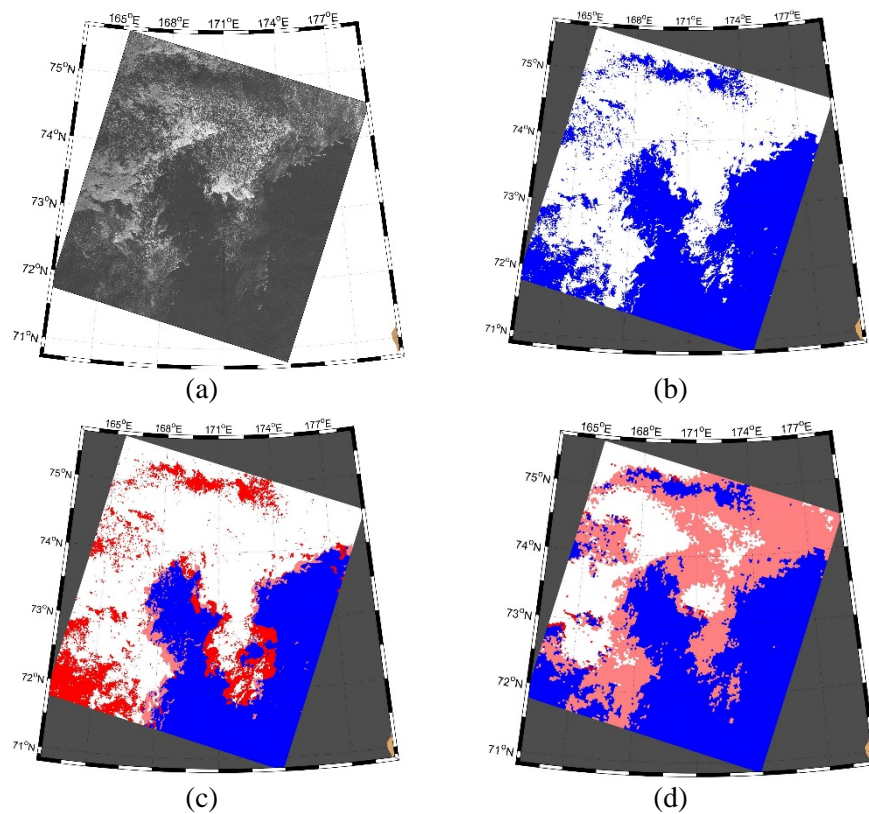
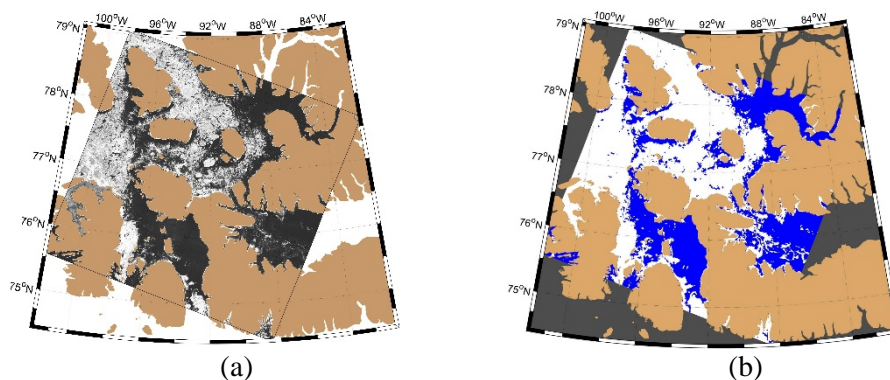


Figure 8. An example of an S1 image (a) and its derived sea ice cover (b) over the area northeast of the East Siberian Sea and its comparison with the IMS (c) and AMSR2 data (d).

3.2.3 Case of the Canadian Arctic Archipelago

Figure 9 shows an image from September 15, 2018, located in the Canadian Arctic Archipelago. This area is mainly covered by land, with sea ice between the straits. Due to the high proportion of land, the total number of matching points is small. Although there are few mismatched points, the *MA* values vary greatly. This phenomenon is the main reason for the low *MA* values in this region. Furthermore, the abnormal phenomena of ice underestimation in the IMS data (see Figure 9c) and the overestimation in the AMSR2 data (see Figure 9d) appear in this image. Presumably, these phenomena are influenced by the surrounding land.



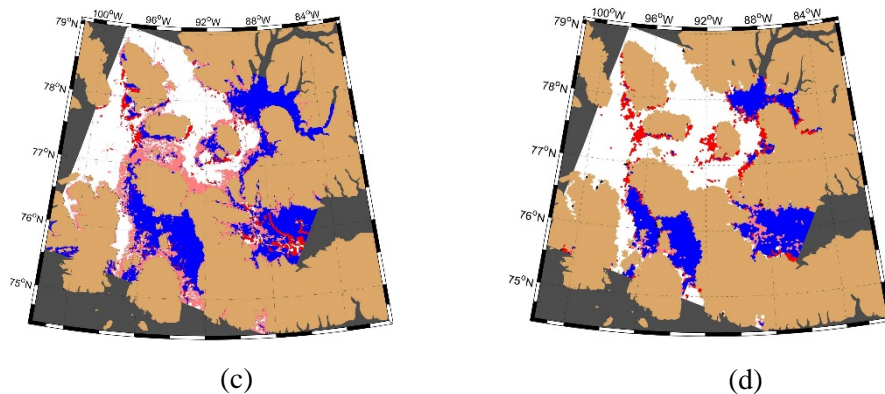


Figure 9. An example of an S1 image (a) and its derived sea ice cover (b) over the CAA and its comparison with the IMS (c) and AMSR2 data (d).

4. Conclusion

In this study, accuracy of the sea ice cover derived from the S1 EW data acquired in summer 2018 was evaluated with two other common sea ice cover datasets: the IMS sea ice cover dataset and the AMSR2 sea ice concentration dataset. The overall matching accuracy between the IMS and SIES1 data is 85.01%, and the overall matching accuracy between the AMSR2 and SIES1 data is 88.69%. Using the S1 SAR imagery for visual validation, the SIES1 produced by our method are the closest to the real ice conditions which can better characterizes the details of marginal ice zone. In addition, the result shows that the IMS dataset mainly overestimates the sea ice cover, while the AMSR2 data relatively underestimates the sea ice cover. Drift (or pack) ice and the regions with high land cover might be the main reasons for the low matching accuracy.

References

- [1] Vihma, Timo. 2014 Effects of Arctic sea ice decline on weather and climate: a review[J]. *Surv. Geophys.*, **35**(5):1175-1214.
- [2] Zhang X, Tu J F, Guo P Q, et al. 2009 The economic estimate of Arctic sea routes and its strategic significance for the development of Chinese economy [J]. *China Soft Science*, **S2**:86-93
- [3] Comiso J C, Cavalieri D J, Markus T. 2004 Sea ice concentration, ice temperature, and snow depth using AMSR-E data[J], **41**(2):243-252.
- [4] Spreen G, Kaleschke L and Heygster G. 2008 Sea ice remote sensing using AMSR-E 89-GHz channels[J]. *J. Geophys. Res.-Atmos.*, **113**(C2).
- [5] Markus, T, Cavalieri, D.J. 2000 An enhancement of the NASA Team sea ice algorithm[J]. *IEEE Trans. Geosci. Remote Sensing*, **38**(3):0-1398.
- [6] Cavalieri, D. J., et al. 1999 Deriving long-term time series of sea ice cover from satellite passive-microwave multisensor data sets[J]. *J. Geophys. Res.*, **104**(C7):15803.
- [7] Hall, D. K. and G. A. Riggs. 2015. MODIS/Aqua Sea Ice Extent Daily L3 Global 1km EASE-Grid Day, Version 6. [Indicate subset used]. Boulder, Colorado USA. NASA National Snow and Ice Data Center Distributed Active Archive Center. doi: <https://doi.org/10.5067/MODIS/MYD29P1D.006>
- [8] Li X-M, Sun Y, Zhang Q, 2019 Extraction of sea ice cover by Sentinel-1 SAR based on machine learning – Part 2: Algorithm development, submitted to *IEEE Trans. Geosci. Remote Sensing*
- [9] Heinrichs, J. F., Cavalieri, D. J. and Markus, T., 2006 Assessment of the AMSR-E sea ice concentration product at the ice edge using RADARSAT-1 and MODIS imagery, *IEEE Trans. Geosci. Remote Sensing*, **44**(11):070-3080
- [10] Parkinson C L, et al. 1999 Arctic sea ice extents, areas, and trends, 1978–1996[J]. *J. Geophys. Res.*, **104**(C9):20837.

- [11] National Ice Center. 2008, updated daily. IMS Daily Northern Hemisphere Snow and Ice Analysis at 1 km, 4 km, and 24 km Resolutions, Version 1. [Indicate subset used]. Boulder, Colorado USA. NSIDC: National Snow and Ice Data Center. doi: <https://doi.org/10.7265/N52R3PMC>. [Date Accessed].
- [12] Spreen, G., L. Kaleschke, and G.Heygster 2008, Sea ice remote sensing using AMSR-E 89 GHz channels *J. Geophys. Res.*, **113**(C2)
- [13] Fetterer, F, et al. 2017, updated daily. Sea Ice Index, Version 3. [Indicate subset used]. Boulder, Colorado USA. NSIDC: National Snow and Ice Data Center. doi: <https://doi.org/10.7265/N5K072F8>.
- [14] Joanna G, Arthur J. M, Edward H. R. "The East Greenland Current." Ocean Surface Currents.. <https://oceancurrents.rsmas.miami.edu/atlantic/east-greenland.html>.

Acknowledgments

The study was partially supported by the National Key Research and Development Program of China (2018YFC1407102). We would also like to thank the European Space Agency for providing the Sentinel-1 data, the University of Bremen for providing the AMSR sea ice concentration dataset and the National Snow & Ice Data Center for providing the IMS data.